

Role of Caspases and CD95/Fas in the Apoptotic Effects of a Nucleotide Analog PMEG in CCRF-CEM Cells

HELENA MERTLÍKOVÁ-KAIEROVÁ, IVAN VOTRUBA,
MARIKA MATOUŠOVÁ, ANTONÍN HOLÝ and MIROSLAV HÁJEK

*Institute of Organic Chemistry and Biochemistry, Academy of Sciences of the Czech Republic, v.v.i.,
Gilead Sciences and IOCB Research Center, Prague, Czech Republic*

Abstract. *Background/Aim:* 9-[2-(phosphonomethoxy)ethyl]guanine (PMEG) is a guanine acyclic nucleotide analog whose targeted prodrugs are being investigated for chemotherapy of lymphomas. Its antiproliferative effects have been attributed to cell cycle arrest and induction of apoptosis, however, the underlying mechanisms remain poorly understood. The objective of this study was to determine the requirements for caspase and CD95/Fas activation in PMEG-induced apoptosis. Additionally, the influence of PMEG on cell cycle regulatory proteins was explored. *Materials and Methods:* CCRF-CEM cells were exposed to PMEG with/without caspase inhibitor or anti-Fas blocking antibody and assayed for phosphatidyl serine externalization, mitochondrial depolarization and the cleavage of procaspase 3 and the nuclear protein poly (ADP-ribose) polymerase (PARP). *Results:* Despite an observed increase of caspase 3, 8 and 9 proteolytic activity, neither pretreatment of the cells with cell-permeable caspase inhibitors nor blocking the death receptor with anti-Fas antibody did prevent apoptosis induced by PMEG. *Conclusion:* PMEG-induced apoptosis is caspase- and CD95/Fas-independent.

9-[2-Phosphonomethoxy)ethyl]guanine (PMEG) is a structural analog of naturally occurring nucleotide dGMP and a member of the family of acyclic nucleoside phosphonates (ANPs). Its potent antiproliferative properties (1) have been largely attributed to the ability of its active metabolite, PMEG diphosphate (PMEGpp), to be incorporated into DNA, inhibit cellular replicative polymerases α , δ and ϵ , and act as a DNA chain terminator (2). Perturbations in the DNA replication process result in an altered cell cycle distribution

(S phase arrest) and induction of apoptosis as observed in several leukemia cell lines (3). Recently, a PMEG prodrug, GS-9219, has been shown to display significant *in vivo* antitumor effects in dogs with spontaneous non-Hodgkin's lymphoma (4). The anticancer activity of a PMEG congener, 9-[(2-phosphonomethoxy)ethyl]-2,6-diaminopurine (PMEDAP), has also been previously described *in vivo* in spontaneous rat T-cell lymphoma (5, 6). Although apoptosis induction appears to play a role in the antitumor activity of PMEG, the underlying molecular mechanisms remain largely unknown.

Caspase activation is a frequent hallmark of apoptosis in many cell types (7). In most cases, caspase-mediated cell death can be assigned to one of two independent pathways: the intrinsic (mitochondrial) cascade or the extrinsic (receptor) pathway. The intrinsic cascade involves mitochondrial depolarization, cytochrome *c* translocation from mitochondria to cytosol and cleavage of procaspase 9 to its active form, while the extrinsic (receptor) pathway requires binding of specific ligands to death receptors (CD95/Fas, TNFR) and is accompanied by caspase 8 activation (8). Both pathways merge while activating the downstream effector caspases (such as 3, 6 or 7) cleaving various nuclear targets.

In the present work, the involvement of caspases and the role of mitochondrial and CD95/Fas pathways in PMEG-induced apoptosis were studied in a T-cell lymphoblastic cell line (CCRF-CEM). In addition, expression of various cyclins, cyclin-dependent kinases (CDKs) and cyclin-dependent kinase inhibitors (CDKIs) were explored in order to explain the molecular basis of cell cycle effects of PMEG and to aid the understanding of how the cell cycle effects contribute to the overall antitumor activity of PMEG.

Correspondence to: Miroslav Hájek, Institute of Organic Chemistry and Biochemistry AS CR, Flemingovo nám. 2, 166 10 Prague 6, Czech Republic. Tel: +420 220183393, Fax: +420 220183560, e-mail: hajek@uochb.cas.cz

Key Words: Acyclic nucleoside phosphonate, programmed cell death, CCRF-CEM cells, cell cycle.

Materials and Methods

Materials. PMEG, was prepared according to Holý (9). The identity and purity of the compound was verified by means of NMR spectroscopy. All other chemicals and materials were obtained from common commercial sources.

Cell culture and proliferation assay. CCRF-CEM cells (ATCC CCL 119) were cultured in RPMI-1640 medium supplemented with 10% (v/v) fetal calf serum, 200 µg/ml of streptomycin, 200 U/ml of penicillin G and 4 mM glutamine under a humidified atmosphere containing 5% CO₂ at 37°C. A total of 10⁵ cells per ml were seeded 24 h prior to an experimental treatment. Where a 6-day incubation was included, cells were subcultured and given fresh media and fresh compound at day 3. Cell proliferation was assessed using Countess® Automated Cell Counter (Invitrogen Ltd, Paisley, UK).

Quantitative RT-PCR. Total RNA from 10⁶ cells was extracted using RNeasy Mini isolation kit (Qiagen GmbH, Hilden, Germany) according to the manufacturer's protocol. The purity of RNA samples was characterized by their 260/280 and 260/230 absorption ratios, which were at least 1.9 and 1.8, respectively. RNA integrity was verified using the Lab-on-a-Chip Agilent 2100 Bioanalyzer (Agilent Technologies, Santa Clara, CA, USA). cDNA was synthesized from 0.5 µg RNA using RT2 First Strand kit (SABiosciences, Frederick, MD, USA) according to the manufacturer's protocol. Human Cell Cycle RT²-Profiler PCR array (SABiosciences) was then used for gene quantification employing DNA Engine Opticon® 2 thermocycler (Biorad, Hercules, CA, USA).

Determination of caspase activity. A total of 10⁷ cells were lysed in 50 mM HEPES buffer pH 7.4, containing 0.3% CHAPS and 5 mM DTT and incubated for 15 min on ice. The 20,000×g supernatant was used for determination of caspase activity using the synthetic colorimetric substrates: *N*-Acetyl-Asp-Glu-Val-Asp-*p*-nitroaniline (Ac-DEVD-pNA; Sigma, St. Louis, MO, USA), *N*-Acetyl-Ile-Glu-Thr-Acp-*p*-nitroaniline (Ac-IETD-pNA; Sigma) and Leu-Glu-His-Asp-*p*-nitroaniline (LEHD-pNA; Merck KGaA, Darmstadt, Germany) for caspase 3, 8 and 9, respectively. Each microplate well contained 80 µl of assay buffer (20 mM HEPES pH 7.4, 0.1% CHAPS, 5 mM DTT, 2 mM EDTA), 10 µl of cell lysate and 10 µl of the respective substrate (final concentration 200 µM). Caspase activity was calculated from the slope of recorded absorbance at 405 nm, which was compared to the standard curve of free pNA (Sigma).

Flow cytometric determination of mitochondrial membrane potential ($\Delta\Psi$). Cells (10⁶) were washed with PBS and resuspended with 1 ml of pre-warmed culture media containing 1 µg/ml of JC-1 dye (5.5', 6.6' -tetrachloro-1.1', 3.3'-tetraethylbenzimidazolyl-carbocyanine iodide). The cells were incubated for 15 min at 37°C after which they were washed twice with PBS and immediately subjected to FACS analysis. The fluorescent cationic dye is accumulated in the mitochondria of polarized ('healthy') cells emitting red fluorescence (590 nm) due to formation of J-aggregates. Depolarized cells are characterized by the presence of monomeric form of the dye in the cytosol where it fluoresces green (527 nm).

Flow cytometric determination of phosphatidyl serine externalization. Phosphatidyl serine externalization in treated cells was quantified using an ApoAlert® Annexin V-FITC apoptosis kit (Clontech Laboratories, Inc, Mountain View, CA, USA). Briefly, 10⁶ cells were washed with PBS and resuspended in 0.2 ml of the Ca²⁺-containing binding buffer supplemented with 1 µg/ml of annexin V-FITC conjugate and incubated for 15 min in the dark. The cells were washed twice with the binding buffer, propidium iodide (5 µg/ml) was added and the cells were immediately subjected to flow cytometric analysis.

Cell cycle analysis. Cells (10⁶) were washed twice with PBS and fixed with 70% ice-cold ethanol for 30 min. Fixed cells were washed in PBS, treated with RNase A (500 µg/ml) for 30 min at 37°C and incubated with a staining solution containing 0.1% Triton X®-100 and propidium iodide (100 µg/ml) in PBS for 1 h. Cellular DNA content was determined using a flow cytometer FACSAria (BD Biosciences, San Jose, CA, USA) and analyzed using ModFit LT 3.0 program (Verity Software House, Topsham, ME, USA).

DNA fragmentation assay. A total of 1.5×10⁶ cells were suspended in 500 µl of lysis buffer (100 mM Tris-HCl, pH 8.0, 10 mM EDTA, 2% SDS) containing 5 µl of proteinase K and incubated for 1 hour at 56°C. 200 µl of 5 M NaCl and 1/10 volume of 3 M sodium acetate were added followed by centrifugation at 15,000×g for 5 min. Supernatant was incubated with RNase A for 30 min, RT and the DNA was precipitated by adding two volumes of absolute ethanol at -20°C overnight. The pelleted DNA was washed twice in 70% ethanol, air-dried and resuspended in 50 µl of TE-buffer (10 mM Tris-HCl, pH 8.0, 1 mM EDTA). 0.6 µg of DNA were subjected to electrophoresis on a 0.7% agarose gel containing ethidium bromide and visualized under UV light.

Western blot analysis. A total of 10⁷ cells were lysed in ice-cold RIPA buffer containing protease and phosphatase inhibitors (Pierce, Rockford, IL, USA) and centrifuged at 20,000×g. 30 µg of total supernatant protein were loaded on a 12% polyacrylamide gel, electrophoresed and electroblotted onto a PVDF membrane. Membranes were blocked in 5% non-fat dry milk (Cell Signaling Technology (CST), Danvers, MA, USA) in TBS containing 0.05% of Tween 20 (Pierce) and probed with anti-PARP or anti-cleaved caspase 3 antibodies (CST) and appropriate HRP-conjugated secondary antibodies (CST). SuperSignal® West Femto Chemiluminescent Substrate (Pierce) was used for signal detection by CCD camera.

Statistical evaluation. Unless otherwise indicated, the data are presented as the mean±SEM from at least three independent experiments. Statistical evaluation was performed using GraphPad Prism version 5.00 for Windows (GraphPad Software, San Diego CA, USA; www.graphpad.com).

Results

PMEG induces concentration- and time-dependent apoptosis in CCRF-CEM lymphoblasts. PMEG-treated cells revealed an early (24 h) inhibition of cell growth, which became even more pronounced at later time points (72 h and 144 h) (Figure 1). Inhibition of cell proliferation by PMEG was concentration-dependent with an approximate GIC₅₀ value of 1 µM at 72 h. The apoptotic hallmarks were evaluated using three different methods: binding of annexin V to the externalized phosphatidyl serine (PS) (Figure 2A), mitochondrial membrane potential measurement with use of JC-1 probe (Figure 2B) and DNA fragmentation assay (Figure 2C). PMEG-induced apoptosis was clearly concentration dependent but, contrary to the inhibition of cell proliferation, the onset of the apoptotic response was rather slow. A close correlation between the mitochondrial depolari-

Table I. Effect of cell permeable pan-caspase inhibitor Z-VAD-FMK on PMEG-induced apoptosis.

	% Shrunken cells	% Cells with low $\Delta\Psi_m$	% Early APO cells	% Late APO/NECRO cells	% NECRO cells
Low PMEG, 72 h					
Control	14±7	11±2	6±1	6±3	7±3
PMEG 5 μ M	38±13	35±5	19±7	22±8	9±7
PMEG 5 μ M + Z-VAD-FMK 20 μ M	39±14	38±6	24±5	20±7	7±5
Z-VAD-FMK 20 μ M	8±3	8±2	4±1	3±0	5±3
High PMEG, 24 h					
Control	14±1	6±0	5±1	7±1	4±1
PMEG 500 μ M	46±1	27±2	34±5	14±0	5±1
PMEG 500 μ M + Z-VAD-FMK 20 μ M	42±1	26±1	33±5	14±2	3±0
PMEG 500 μ M + Z-VAD-FMK 100 μ M	38±4	32±5	10±1*	27±3**	7±1
Z-VAD-FMK 100 μ M	7±0	nd	4±0	4±0	4±1

* $p<0.05$ vs. PMEG only treated control, ** $p<0.01$ vs. PMEG. The data are expressed as means of three independent experiments±SD. Analysis of cell shrinkage was based on a decrease in their forward-angle light scatter (FSC) represented as a cluster shift on FSC vs. SSC (side-angle light scatter) dot plots. APO: Apoptosis; NECRO: necrotic.

zation and PS externalization indicated the involvement of mitochondria in the apoptosis induction.

Caspases are activated but not required for PMEG-induced apoptosis in CCRF-CEM cells. PMEG increased catalytic activity of caspase 8 and 9 and especially caspase 3 in CCRF-CEM cells (Figure 2D). Both initiator caspase 8 and 9 are therefore likely to contribute to the executioner caspase 3 activation upon PMEG treatment. Whereas the absolute activity of caspase 8 in PMEG-treated cells was greater than that of caspase 9, the relative increase in caspase 9 activity was more substantial (160 and 330% for caspase 8 and 9, respectively), indicating a preferential role of the intrinsic (mitochondrial) pathway.

To assess the role of caspases in PMEG-induced apoptosis, CCRF-CEM cells were pre-incubated with a cell permeable broad-spectrum caspase inhibitor *N*-benzyloxycarbonyl-Val-Ala-Asp(O-Me) fluoromethyl ketone (Z-VAD-FMK) prior to PMEG treatment. No significant diminution of the major apoptotic markers was found in the inhibitor-pretreated cells compared to the cells treated with PMEG only irrespective of experimental setup employed (Table I). Neither the standard (72 h) incubation of the cells with moderate concentrations of PMEG, nor a short-term treatment (24 h) with high PMEG and inhibitor concentrations resulted in apoptosis diminution, although the caspase catalytic activity was shown to be inhibited (Figure 3). Not even the cleavage of procaspase 3 to its active form was completely blocked by Z-VAD-FMK or more specific inhibitors of caspase 8 and 9, benzyloxycarbonyl-Ile-Glu-Thr-Asp fluoromethyl ketone (Z-IETD-FMK) and benzyloxycarbonyl-Leu-Glu-His-Asp fluoromethyl ketone (Z-LEHD-FMK), respectively (Figure 4).

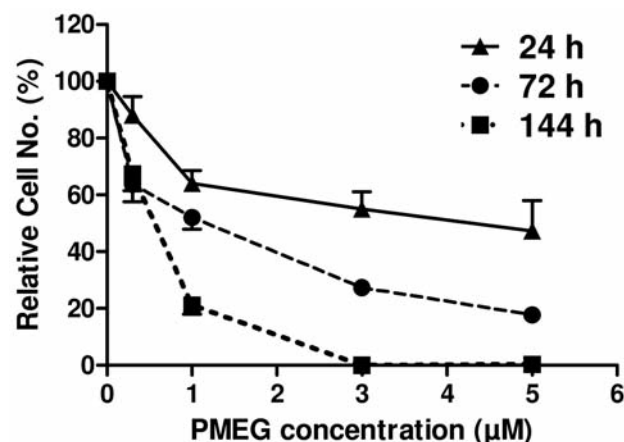


Figure 1. PMEG-induced inhibition of cell proliferation in CCRF-CEM cells. Cells were incubated for 24, 72 and 144 h with 0–5 μ M PMEG at 37°C with subculturing and renewing the medium at 72 h wherever longer exposures were performed. At the end of incubation period viable cells were counted under a light microscope following Trypan blue staining. The data are given as a mean percentage of control cells±SEM from at least three independent experiments. All data points, except for 0.3 μ M at 24 h, were found to differ statistically from the respective untreated control at $p<0.01$ (one-way ANOVA with Dunnett's multiple comparison post-test).

On the other hand, the cleavage of poly(ADP-ribose) polymerase (PARP), a downstream target of caspase 3, was inhibited by Z-VAD-FMK in a concentration-dependent manner but not by Z-IETD-FMK and Z-LEHD-FMK. It is also evident that PMEG not only induced the cleavage of PARP but also up-regulated PARP protein and that caspase inhibitors, especially Z-VAD-FMK, partially prevented this effect.

Table II. Expression of various cyclins, CDKs and CDKIs in CCRF-CEM cells following PMEG treatment (1 μ M, 72 h).

Gene symbol	Description	n	p-Value	Fold regulation
<i>CCNA1</i>	Cyclin A1	2	0.876	1.20
<i>CCNA2</i>	Cyclin A2	2	0.850	-1.05
<i>CCNB1</i>	Cyclin B1	2	0.990	1.00
<i>CCNB2</i>	Cyclin B2	2	0.688	1.06
<i>CCND1</i>	Cyclin D1	2	0.926	1.07
<i>CCND2</i>	Cyclin D2	2	0.638	-1.74
<i>CCND3</i>	Cyclin D3	2	0.850	1.12
<i>CCNE1</i>	Cyclin E1	3	0.011	2.48
<i>CDC42</i>	Cell division cycle 42 (GTP-binding protein 25 kDa)	2	0.642	1.07
<i>CDC25A</i>	Cell division cycle 25 homolog A (<i>S. pombe</i>)	3	0.799	1.02
<i>CDK2</i>	Cyclin-dependent kinase 2	3	0.563	1.17
<i>CDK4</i>	Cyclin-dependent kinase 4	3	0.211	1.32
<i>CDK6</i>	Cyclin-dependent kinase 6	2	0.428	1.47
<i>CDKN1A</i>	Cyclin-dependent kinase inhibitor 1A (p21)	3	0.471	1.86
<i>CDKN1B</i>	Cyclin-dependent kinase inhibitor 1B (p27)	2	0.658	1.34
<i>CDKN1C</i>	Cyclin-dependent kinase inhibitor 1C (p57)	2	0.934	1.07
<i>CDKN2A</i>	Cyclin-dependent kinase inhibitor 2A (p16)	3	0.514	-1.25
<i>CDKN2B</i>	Cyclin-dependent kinase inhibitor 2B (p15)	2	0.778	1.43
<i>CDKN2C</i>	Cyclin-dependent kinase inhibitor 2C (p18)	2	0.315	1.50
<i>CDKN2D</i>	Cyclin-dependent kinase inhibitor 2D (p19)	2	0.765	1.19

Data analysis including statistical evaluation was performed with use of a VBA applet freely available at PCR Array Data Analysis Web Portal: <http://www.SABiosciences.com/pcrarraydataanalysis.php>

PMEG-induced apoptosis is independent of CD95/Fas receptor signaling. To investigate the contribution of Fas-receptor signaling to PMEG-induced apoptosis, the CCRF-CEM cells were pre-incubated with anti-Fas blocking antibody (clone ZB4) prior to PMEG treatment. The data on PS exposure, $\Delta\Psi_m$ and DNA fragmentation demonstrate that blocking Fas receptor prior to PMEG treatment did not diminish the extent of cell death (Figure 5), thus excluding the involvement of Fas-receptor pathway in the apoptotic effects of PMEG. In contrast, the activity of anti-Fas activating antibody (clone CH11) that induces the apoptosis by stimulating Fas receptor was nearly completely prevented by anti-Fas blocking antibody.

PMEG-induced S phase arrest is accompanied by the elevation of cyclin E1 gene expression. Incubation of the cells with increasing concentration of PMEG reduced the proportion of cells in G₁/G₀ phase while simultaneously increasing the accumulation of cells in S phase (Figure 6). This effect was clearly concentration-dependent while being less dependent on the incubation period. Following a 72-hour incubation with 1 μ M PMEG, a significant, >2-fold increase in the expression of *cyclin E1* gene was found, but not genes encoding other cyclins, CDKs, and CDKIs (Table II).

Discussion

Determining the involvement of caspases in chemotherapy-induced apoptosis is essential for understanding its mechanism of action and may have implications for predicting its clinical efficacy and resistance to the therapy. The role of caspases has been recently implicated in apoptosis induced by an adenine analog cladribine (2-CdA) in Jurkat cells (10). In an independent study, both caspase-dependent and independent mode of cell death have been identified in JM-1 and Jurkat cells treated with 2-CdA (11). To date, there has been no data on the contribution of caspases to the apoptosis induced by PMEG or other acyclic nucleoside phosphonates. In this study, it is shown for the first time that in T-cell derived CCRF-CEM leukemia cells PMEG induces apoptosis that is not entirely dependent on caspases, although caspases are clearly activated following PMEG treatment. These data point to the key role of mitochondrial membrane depolarization (loss of $\Delta\Psi_m$), which was virtually unaffected by caspase inhibition consistently with findings of Marzo *et al.* (11) for cladribine-induced apoptosis. It has been suggested before that the cells co-incubated with apoptotic stimuli and caspase inhibitor Z-VAD-FMK might eventually switch from apoptosis to necrosis (12). While this does not appear to be the case for

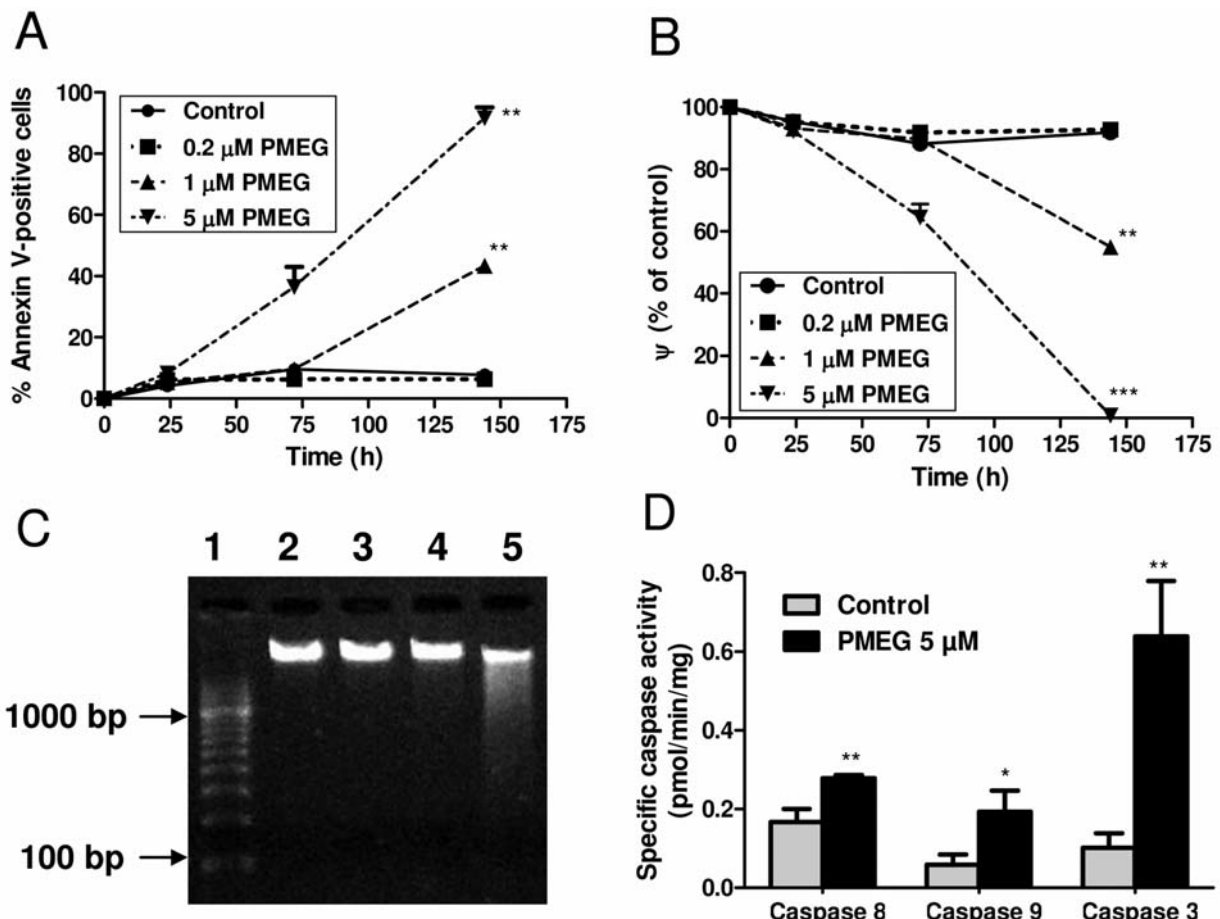


Figure 2. Induction of apoptosis and caspase activation in PMEG-treated CCRF-CEM cells. Cells were incubated with 0-5 μ M PMEG for indicated period of time and subjected to annexin V-staining (A), JC-1 staining (B), DNA fragmentation assay (C) and caspase activity determination (D). The data are given as means from at least three independent experiments \pm SEM with exception of C, which is a representative of two separate experiments at 72 h (1, 100 bp marker; 2, Control; 3, 0.2 μ M PMEG; 4, 1 μ M PMEG; 5, 5 μ M PMEG). * p <0.05, ** p <0.01, *** p <0.001 compared with untreated cells (Student's *t*-test).

PMEG at standard concentration (5 μ M), increased PI-positivity was observed in cells treated with high concentration of PMEG (500 μ M) and Z-VAD-FMK (100 μ M). In accordance with the data on fludarabine-induced apoptosis in chronic lymphocytic leukemia cells (13), this study observed a marked inhibition of PARP up-regulation and activation in CCRF-CEM cells pretreated with Z-VAD-FMK prior to PMEG exposure. PARP is a downstream target of caspase 3 although it is also known to be activated in a caspase-independent manner (14). PARP activation in response to PMEG appears to be largely caspase-dependent and not absolutely essential for PMEG-induced apoptosis.

Due to the apparent lack of selectivity of fluoromethyl ketone (FMK) inhibitors towards their respective caspases (15) this study opted to elucidate the relative contribution of mitochondrial and receptor apoptotic pathway by means of anti-Fas blocking antibody (clone ZB4), which inactivates

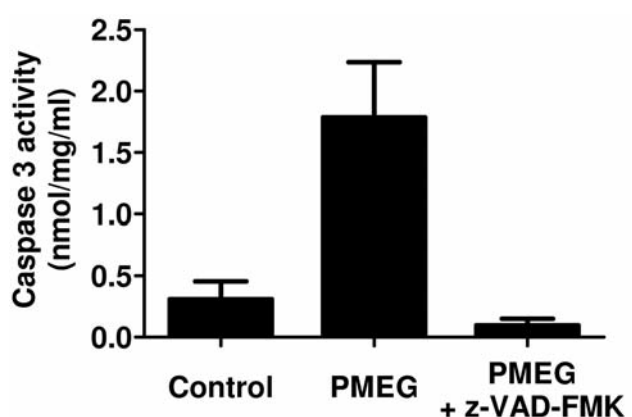


Figure 3. Effect of pan-caspase inhibitor Z-VAD-FMK on PMEG-induced caspase 3 activity in cell lysates. CCRF-CEM cells were incubated for 72 h with 0 (control), 5 μ M PMEG and 5 μ M PMEG after pre-incubation with 20 μ M Z-VAD-FMK.

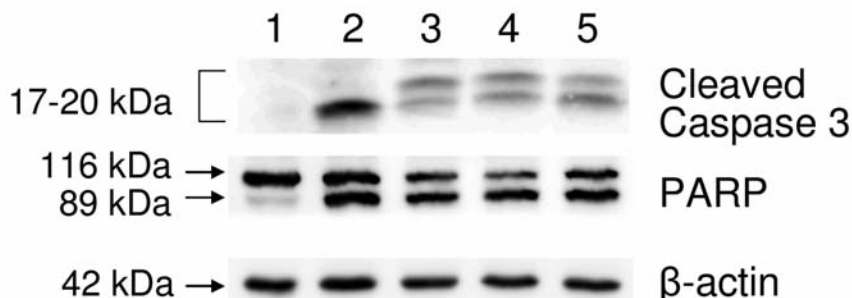
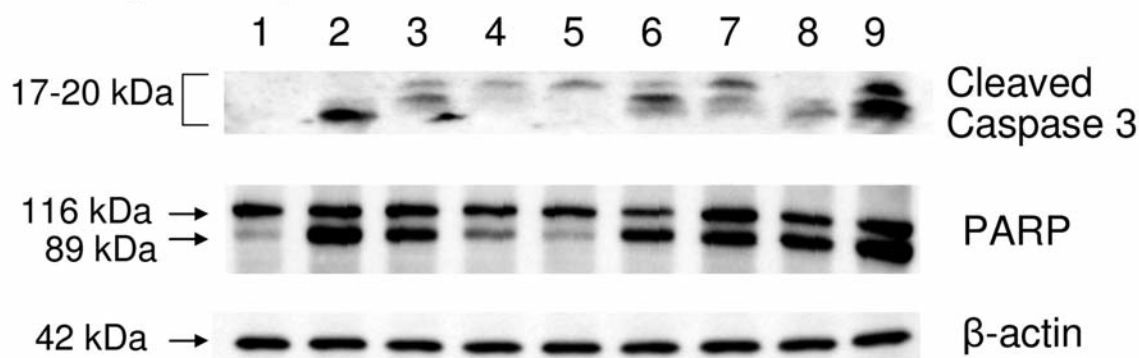
A - Low PMEG, 72 h**B - High PMEG, 24 h**

Figure 4. Inhibition of procaspase 3 and PARP cleavage by cell-permeable caspase inhibitors. Immunoblotting was performed as described in Materials and Methods. Results are representative of two independent experiments. A: 72 h exposure, 3 μM PMEG, 20 μM inhibitor: 1, Control; 2, PMEG; 3, PMEG+Z-VAD-FMK; 4, PMEG+Z-IETD-FMK; 5, PMEG+Z-LEHD-FMK. B: 24 h exposure, 500 μM PMEG, 20-100 μM inhibitor: 1, Control; 2, PMEG; 3, PMEG+20 μM Z-VAD-FMK; 4, PMEG+50 μM Z-VAD-FMK; 5, PMEG+100 μM Z-VAD-FMK; 6, PMEG+20 μM Z-IETD-FMK; 7, PMEG+100 μM Z-IETD-FMK; 8, PMEG+20 μM Z-LEHD-FMK; 9, PMEG+100 μM Z-LEHD-FMK.

Fas receptor and its downstream effectors. It has been previously proposed that 2-CdA-induced apoptosis is mediated by the Fas/Fas-L pathway in MOLT-4 cells (16) while others showed the opposite (17). As no prevention of PMEG-induced apoptosis under the conditions of Fas-receptor blockade was found, it seems that the apoptosis by PMEG in CCRF-CEM cells is CD95/Fas-independent and depends rather on the intrinsic mitochondrial pathway. These data are in agreement with a higher relative activation of caspase 9 over caspase 8 in PMEG-treated cells and the observed mitochondrial depolarization being one of the first hallmarks of PMEG-induced apoptosis.

The apparent lack of a typical oligonucleosomal DNA fragmentation combined with the fact that caspase inhibitor did not prevent PMEG-induced apoptosis indicated that it might be initiated by the caspase-independent mitochondrial-nuclear translocation of apoptosis-inducing factor (AIF). Although AIF translocation was indeed detected in some

PMEG-treated cells (by use of immunofluorescence microscopy), the relative frequency of AIF-positive cells was less than 10% (data not shown). It is therefore unlikely that release of AIF from mitochondria would play a major role in PMEG-induced apoptosis in CCRF-CEM cells.

Investigations of PMEG effects on cell cycle progression in the CCRF-CEM cells indicated that the S phase arrest contributes to the early inhibition of cell growth that precedes induction of apoptosis. The effect of PMEG on the expression of 20 representative cyclins, cyclin-dependent kinases and their inhibitors was evaluated, but the only gene found to be significantly up-regulated was *cyclin E1* (2.5-fold). This cyclin interacts with CDK2 and is responsible for the transition of cell cycle from G₁ to S phase (18), which is in accordance with the current findings. Unlike others who characterized the adenine analog of PMEG (*i.e.* PMEA) in MOLT-4 cells, no changes were detected in the expression of cyclin A or cyclin B1 (19).

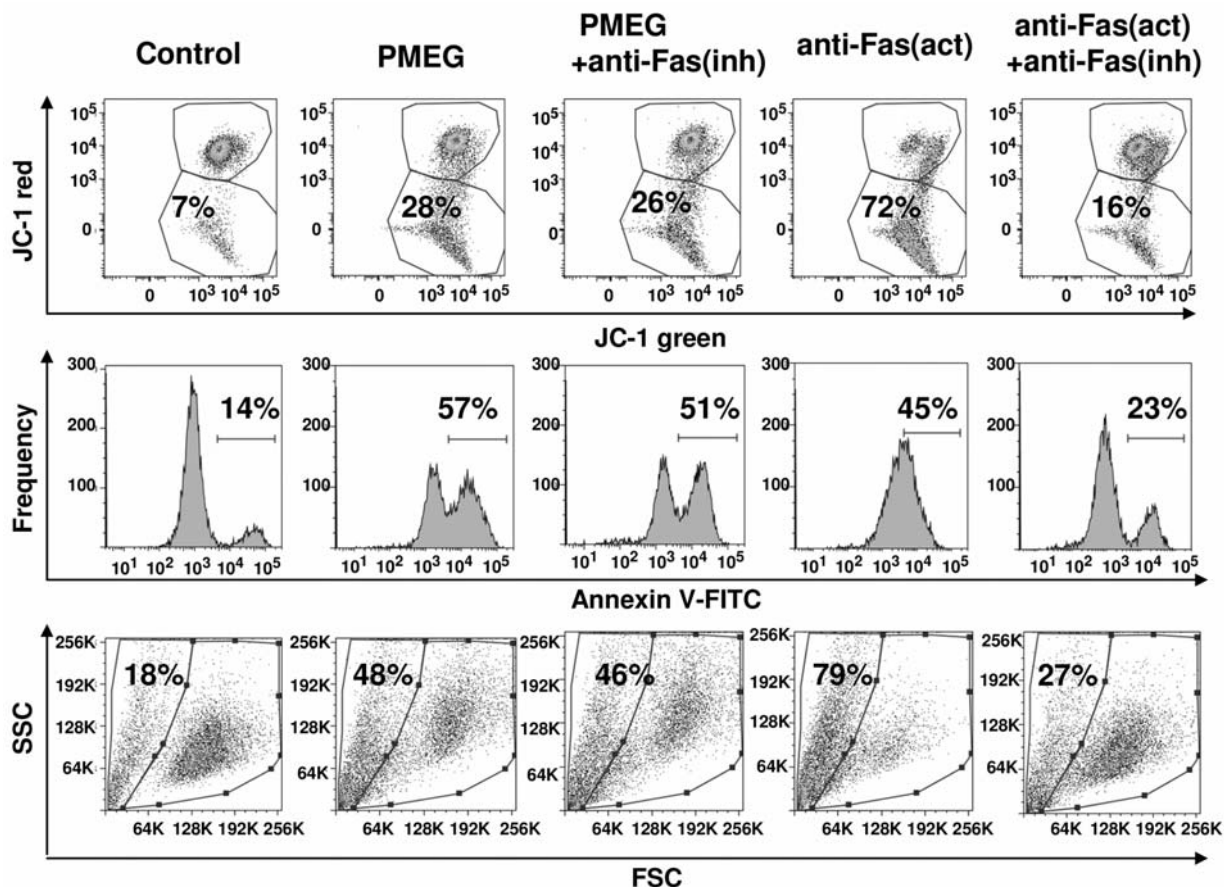


Figure 5. Anti-Fas blocking antibody does not prevent PMEG-induced apoptosis. Row 1: mitochondrial membrane potential of JC-1-stained cells; Row 2: Annexin V-FITC stain of externalized phosphatidyl serine of apoptotic cells; Row 3: shrunken apoptotic morphology indicated by a decrease in FSC signal. Functionality of the assay was verified using anti-Fas activating antibody (clone CH11) with/without anti-Fas blocking antibody (clone ZB4).

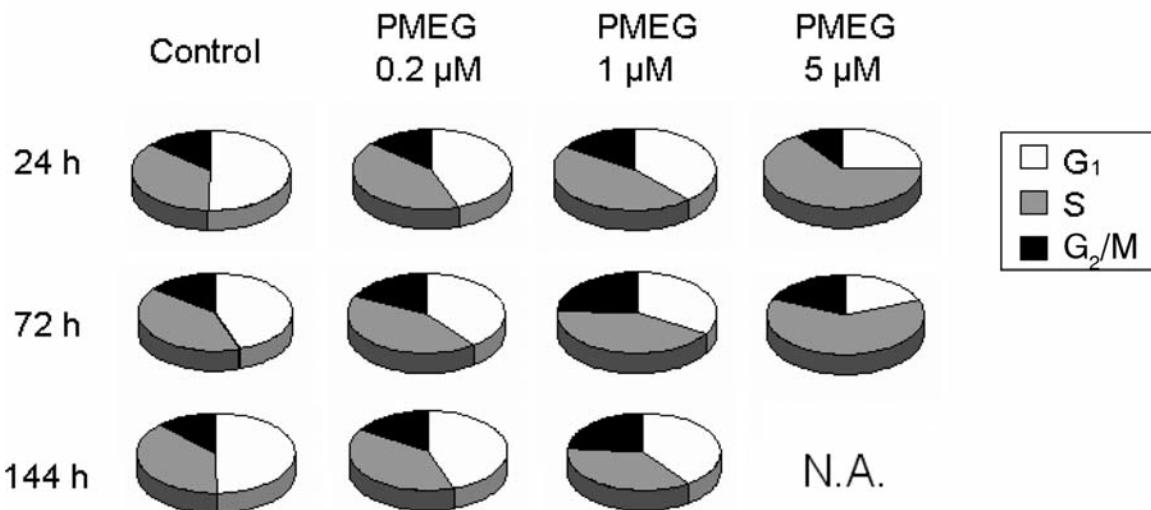


Figure 6. Effect of PMEG on cell cycle distribution. CCRF-CEM cells were incubated for 24, 72 and 144 h with 0 (control), 0.2, 1, and 5 μM PMEG and subjected to flow cytometric DNA content analysis.

In conclusion, this study showed that PMEG-induced apoptosis is accompanied by activation of caspases. These, however, do not appear to be required for the execution of PMEG-induced apoptosis in CCRF-CEM cells, possibly because the cells compensate for a blocked caspase pathway by switching to caspase-independent mechanisms or necrotic cell death. These findings indicate that caspase functionality and/or expression status is unlikely to affect the antitumor efficacy of PMEG and its prodrug GS-9219 in T-cell-derived leukemias. This should be verified and further explored by characterizing the mechanisms of PMEG-induced cell death in a broader range of malignant lymphoid cells.

Acknowledgements

This work was conducted as part of a research project of the Institute (OZ40550506) and the Centre for New Antivirals and Antineoplastics by the Ministry of Education, Youth and Sports of the Czech Republic #1M0508. The Authors would like to thank Tomas Cihlar for his revisions and valuable advice.

References

- 1 Holý A: Phosphonomethoxyalkyl analogs of nucleotides. *Curr Pharm Des* 9: 2567-2592, 2003.
- 2 Kramata P, Votruba I, Otová B and Holý A: Different inhibitory potencies of acyclic phosphonomethoxyalkyl nucleotide analogs toward DNA polymerases. *Mol Pharmacol* 49: 1005-1011, 1996.
- 3 Franěk F, Holý A, Votruba I and Eckslager T: Acyclic nucleotide analogues suppress growth and induce apoptosis in human leukemia cell lines. *Int J Oncol* 14: 745-752, 1999.
- 4 Reiser H, Wang J, Chong L, Watkins WJ, Ray AS, Shibata R, Birkus G, Cihlar T, Wu S, Li B, Liu X, Henne IN, Wolfgang GH, Desai M, Rhodes GR, Fridland A, Lee WA, Plunkett W, Vail D, Thamm DH, Jeraj R and Tumas DB: GS-9219-a novel acyclic nucleotide analogue with potent antineoplastic activity in dogs with spontaneous non-Hodgkin's lymphoma. *Clin Cancer Res* 14: 2824-2832, 2008.
- 5 Otová B, Francová K, Franěk F, Koutník P, Votruba I, Holý A, Sladká M and Schramlová J: 9-[2-(Phosphonomethoxyethyl]-2,6-diaminopurine (PMEDAP), a potential drug against hematological malignancies, induces apoptosis. *Anticancer Res* 19: 3173-3182, 1999.
- 6 Valeriánová M, Otová B, Bílá V, Hanzalová J, Votruba I, Holý A, Eckslager T, Krejčí O and Trka J: PMEDAP and its N⁶-substituted derivatives: genotoxic effect and apoptosis in *in vitro* conditions. *Anticancer Res* 23: 4933-4939, 2003.
- 7 Smolewski P, Darzynkiewicz Z and Robak T: Caspase-mediated cell death in hematological malignancies: theoretical considerations, methods of assessment, and clinical implications. *Leuk Lymphoma* 44: 1089-1104, 2003.
- 8 Chen M and Wang J: Initiator caspases in apoptosis signaling pathways. *Apoptosis* 7: 313-319, 2002.
- 9 Holý A: Synthesis of acyclic nucleoside phosphonates. *Curr Protoc Nucleic Acid Chem Chapter 14: Unit 14.2*, 2005.
- 10 Conrad DM, Robichaud MR, Mader JS, Boudreau RT, Richardson AM, Giacomantonio CA and Hoskin DW: 2-Chloro-2'-deoxyadenosine-induced apoptosis in T leukemia cells is mediated via a caspase-3-dependent mitochondrial feedback amplification loop. *Int J Oncol* 32: 1325-1333, 2008.
- 11 Marzo I, Pérez-Galán P, Giraldo P, Rubio-Félix D, Anel A and Naval J: Cladribine induces apoptosis in human leukaemia cells by caspase-dependent and -independent pathways acting on mitochondria. *Biochem J* 359: 537-546, 2001.
- 12 Hirsch T, Marchetti P, Susin SA, Dallaporta B, Zamzami N, Marzo I, Geuskens M and Kroemer G: The apoptosis-necrosis paradox. Apoptogenic proteases activated after mitochondrial permeability transition determine the mode of cell death. *Oncogene* 15: 1573-1581, 1997.
- 13 Pettitt AR and Cawley JC: Caspases influence the mode but not the extent of cell death induced by purine analogues in chronic lymphocytic leukaemia. *Br J Haematol* 109: 800-804, 2000.
- 14 van Wijk SJ and Hageman GJ: Poly(ADP-ribose) polymerase-1 mediated caspase-independent cell death after ischemia/reperfusion. *Free Radic Biol Med* 39: 81-90, 2005.
- 15 Pereira NA and Song Z: Some commonly used caspase substrates and inhibitors lack the specificity required to monitor individual caspase activity. *Biochem. Biophys. Res Commun* 377: 873-877, 2008.
- 16 Nomura Y, Inanami O, Takahashi K, Matsuda A and Kuwabara M: 2-Chloro-2'-deoxyadenosine induces apoptosis through the Fas/Fas ligand pathway in human leukemia cell line MOLT-4. *Leukemia* 14: 299-306, 2000.
- 17 Klöpfer A, Hasenjäger A, Belka C, Schulze-Osthoff K, Dörken B and Daniel PT: Adenine deoxynucleotides fludarabine and cladribine induce apoptosis in a CD95/Fas receptor, FADD and caspase-8-independent manner by activation of the mitochondrial cell death pathway. *Oncogene* 23: 9408-9418, 2004.
- 18 Möröy T and Geisen C: Cyclin E. *Int J Biochem Cell Biol* 36: 1424-1439, 2004.
- 19 Hatse S, Schols D, De Clercq E and Balzarini J: 9-(2-Phosphonylmethoxyethyl)adenine induces tumor cell differentiation or cell death by blocking cell cycle progression through the S phase. *Cell Growth Differ* 10: 435-446, 1999.

Received April 7, 2010
 Revised May 13, 2010
 Accepted June 1, 2010